CIVIL AND ENVIRONMENTAL ENGINEERING REPORTS

No. 10 2013

TWO-SCALE MODELLING OF REACTIVE POWDER CONCRETE. PART I: REPRESENTATIVE VOLUME ELEMENT AND SOLUTION OF THE CORRESPONDING BOUNDARY VALUE PROBLEM

Arkadiusz DENISIEWICZ*, Mieczysław KUCZMA
University of Zielona Góra,Department of Structural Mechanics,
Institute of Building Engineering
Szafrana st 1, 65-516 Zielona Góra, Poland

The article is the first part of a series concerned with the modelling of reactive powder concrete by using a numerical homogenization technique. This technique is a multi-scale modelling approach. Specifically, in this paper a two scale modelling concept was applied. A model of reactive powder concrete (RPC) is considered whose behaviour on the macro scale is described on the basis of the phenomena occurring in the microstructure of the material. This approach provides the ability to take into account some complex phenomena occurring in the microstructure and their influence on the macroscopic physical and mechanical properties of the material. The method does not require knowledge of the constitutive equation parameters at the macro level. These are determined implicitly for each load increment on the basis of numerical model of a representative volume element (RVE), which reflects the geometrical layout of particular material phases, their constitutive relations and mutual interactions. In this paper the linearly elastic behaviour of each constituent material is assumed within the small strain range. In solving the boundary value problems formulated on the RVE for RPC, the finite element method was utilized. A number of numerical test examples were solved which illustrate the influence of inhomogeneities on the overall response.

Keywords: multiscale modelling, RPC, micro-scale, macro-scale, RVE, computational homogenization, FEM

1. INTRODUCTION

Reactive powder concrete (RPC) is currently one of the most modern building materials created on the basis of cement [2]. RPC is included in the class of

* Corresponding author. E-mail: a.denisiewicz@ib.uz.zgora.pl

ultrahigh value concretes with the resistance to compression compared to steel. They are also classified as composites with cement matrix of ultrahigh resistance properties, and are often called the low-temperature ceramics. Thanks to the high resistance and ductility of RPC concrete, we can significantly reduce the weight and cross-sectional dimensions of structures built from it, while simultaneously the designer is given a larger freedom in providing the structure with the fine architectural expression and in overcoming significant spans. By virtue of the good physical and mechanical properties of reactive powder concrete, it finds a wide interest not only as the construction material, but also as the cladding material for houses and other buildings, and even as a material for furniture making (Fig.1).

Fig. 1. Examples of applications of reactive powder concrete [9]: a) elevation of the Bus Centre in Thiais France, b) roofing at the railway station in Calgary, c) a table

As an effective compuatational tool for determing and testing the material properties of RPC concrete and for the needs of the static-strength analysis of building and engineering constructions made of RPC, we have developed a two-scale model of reactive powder concrete. The modelling approach used is based upon the concept of representative volume element (RVE) and numerical homogenization and leads to a complex computational procedure, so we decided

to divide its presentation into two parts. In this first part, we shall discuss the fundamental features of the microstructure of reactive powder concrete (Sect. 3) and shall present the algorithm of numerical homogenization in the context of solving the boundary value problem formulated for the RVE of RPC. Here all the constituents of RVE are assumed to behave linearly elastic.

In Section 2 we skatch out the idea of computational homogenization. In Sections 3 and 4 the characteristic properties of the RPC microstructure and the corresponding RVE are outlined. The FEM approximation and the BVP posed on the RVE are defined in Sections 5 and 6, and numerical results in Section 7.

2. COMPUTATIONAL HOMOGENIZATION

The concept of computational homogenization is diagrammatically illustrated in Fig. 2. In the method of two-scale numerical homogenization, one determines the response of a material at the macro-scale through an analysis of the material's micro-structure. On the micro-scale level the distributions of micro-stresses and micro-strains are calculated, which via homogenization provide information on the distributions of overaged macroscopic quantities. The whole micro-analysis is carried out on the so-called representative volume element. This is the volume assigned to a material point that is representative for a small surrounding of the point. When the characteristic microscopic length is one order smaller than the characteristic macroscopic length, we can take into consideration only effects of the first order. In case of the RPC concrete, this condition is fulfilled. We can assume that the characteristic dimension in micro-scale is that of the fraction of ground quartz of 0.2 mm. While in the macro-scale it is the dimension of the cross-section of the construction element, e.g. 0.2 x 0.2 m. The numerical homogenization procedure is multistage and computationally complicated [3,4].

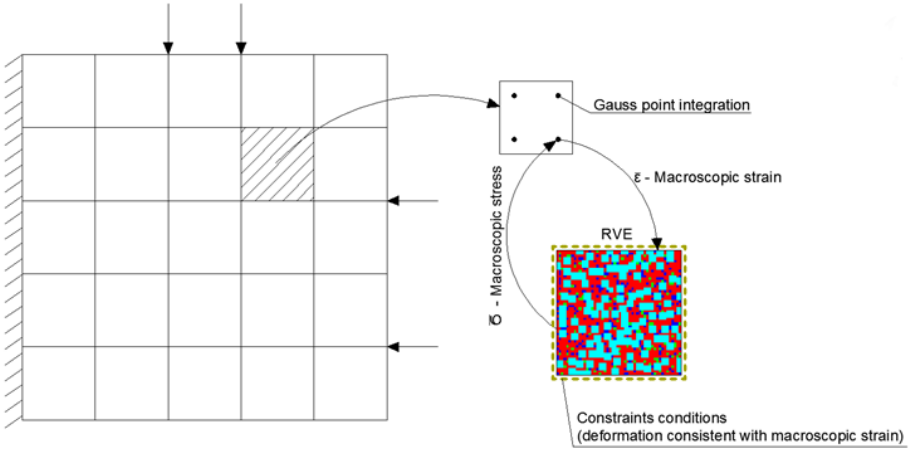

Fig. 2. Idea of two-scale numerical homogenization

3. MICROSTRUCTURE OF REACTIVE POWDER CONCRETE

Reactive powder concrete is invented with the aim of eliminating the faults of the traditional concrete, which is especially achieved by minimizing its porosity to the level of about 4%, by:

- using aggregates with granulation enabling the maximal packaging of components,
- potentially maximal reduction of the water-cement index, with simultaneous application of super-plasticizers,
- applying treatments of pressing in the initial period of the adhesive bonding process.

The improvement of physical and mechanical properties is also obtained by modifying the microstructure of the adhesive matrix by using the proper heat treatment and thanks to using fillers of very small grains, e.g., ground quartz and silica dust. Contrary to the traditional concrete, where the aggregate is the reinforcing element but usually a chemically passive component, the micro-aggregate in RPC concrete, which are usually quartz powders, exhibits the pozzolanic activity. Two characteristic features of the RPC microstructure should be mentioned [6]:

- very compact microstructure of the C-S-H phase
- very good adhesion of the C-S-H phase to mineral inclusions in the form of powder grains and quartz sand and fibers

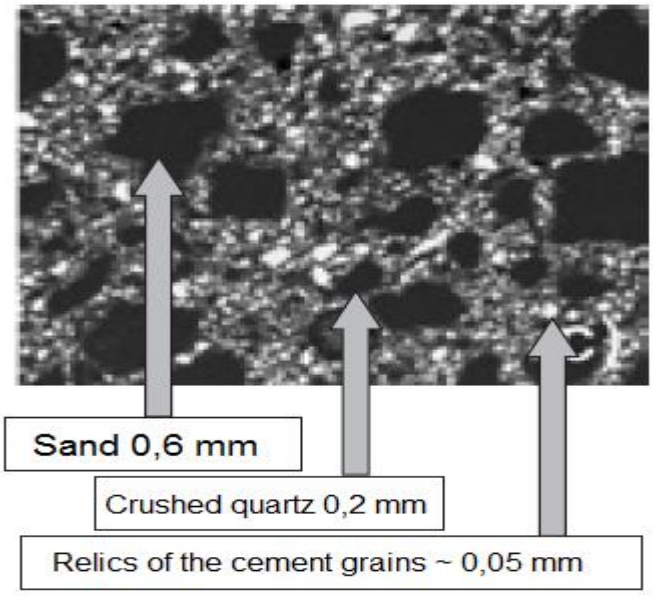

Fig. 3. Microstructure of reavtive powder concrete zoom 200x [6]

4. REPRESENTATIVE VOLUME ELEMENT

In order to model the microstructure of RPC concrete with the composition as in Table 1, in the first approximation step a two-dimensional representative volume element (RVE) was assumed. RVE is modelled with the help of the finite element method. In the calculations we have divided a square RVE into 2500 finite elements, each with the size of 0.2 x 0.2 mm, i.e. each side of RVE of the length of 10 mm is split into 50 equal finite intervals. A representative composition of reactive powder concrete is listed in Tab. 1.

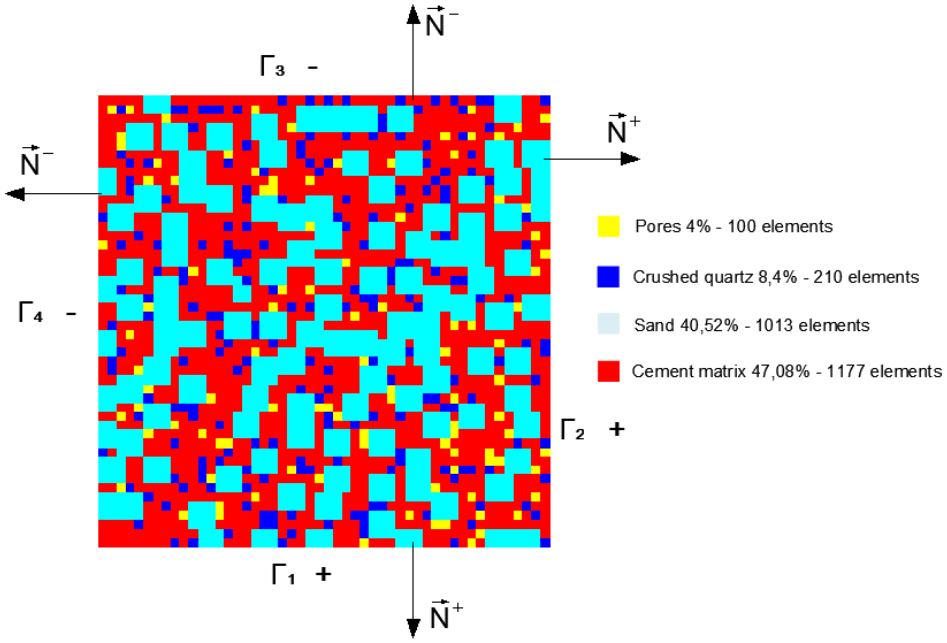

Fig. 4. Representative Volume Element (2D): cement matrix (red colour), sand of grain size to 0.6 mm (cyan colour), crushed quartz of grain size to 0.2 mm (blue colour), pores (yellow green colour)

Table 1. Representative composition of RPC concrete

Component	Volume [kg/m3]	Mass percentage [%]
Cement	705	28,20
Silica fume	230	9,20
Crushed quartz	210	8,40
Sand	1013	40,52
Superplasticizer	17	0,68
Steel fibers	140	5,60
Water	185	7,40

Because of the random character of the arrangement of concrete's components, a stochastic approach to generating the RVE structure was applied (Fig. 4). Building the structure consists of the random selection of an element (from the 50x50 grid) and then also of the random assignment of a component (pores, crushed quartz, sand, cement matrix) to the selected position. The basic size of the RVE component was assumed to be equal of 0.2 mm. In case of drawing the sand component, the process of arranging elements of the grid takes place according to the scheme shown in Fig. 5, which takes into account the maximal size of the grain of 0.6 mm. The extreme locations correspond to the smaller grains of the same component.

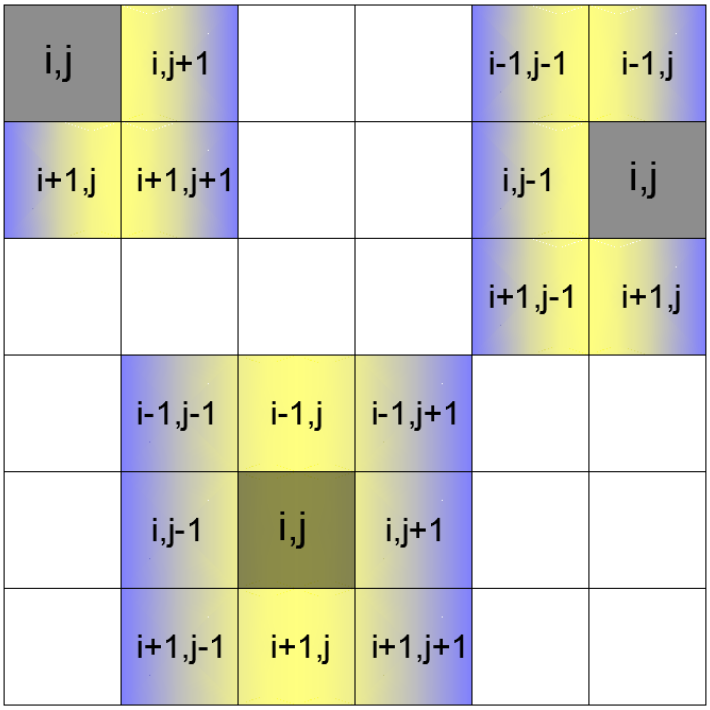

Fig. 5. Principle of generating a RVE structure

For generating the total pseudo-random integer number γ_{n+1} from the intervals of <1,4> (number of component) and of <1,50> (position of component) there was applied a generator

$$\gamma_{n+1} = \text{int}\,(x + (y - x + 1) \cdot X_{n+1}) \tag{4.1}$$

where x is the left endpoint of the range of drawing and y is the right endpoint of the range of drawing, and

$$
\begin{aligned}
&X_{n+1} = (aX_n + b) \bmod c \\
&a = 7^5 = 16807 \quad b = 0 \\
&c = 2^{31} - 1 = 2147483647
\end{aligned}
\tag{4.2}
$$

It is the affine generator of pseudo-random numbers from the range of <0,1>. The whole procedure of building the structure of the represented volume element is performed by a computer programme written in the FORTRAN 90 language in which the libraries [7,8] were used.

5. FINITE ELEMENT METHOD IN COMPUTATIONAL HOMOGENIZATION

For solving the boundary value problems at the macro and micro scales, the classical displacement version of the finite element method was applied. The 2D domain under consideration Ω was discretized by means of the four node finite element Q4 with two degrees of freedom at each node. The horizontal $u = u(\xi,\eta)$ and vertical $v = v(\xi,\eta)$ components of displacement field $\mathbf{u}$ are approximated with the bilinear shape functions

$$
\begin{aligned}
&N_1(\xi,\eta) = \frac{1}{4}(1-\xi-\eta+\xi\eta) \quad N_2(\xi,\eta) = \frac{1}{4}(1+\xi-\eta-\xi\eta) \\
&N_3(\xi,\eta) = \frac{1}{4}(1+\xi+\eta+\xi\eta) \quad N_4(\xi,\eta) = \frac{1}{4}(1-\xi+\eta-\xi\eta)
\end{aligned}
\tag{5.1}
$$

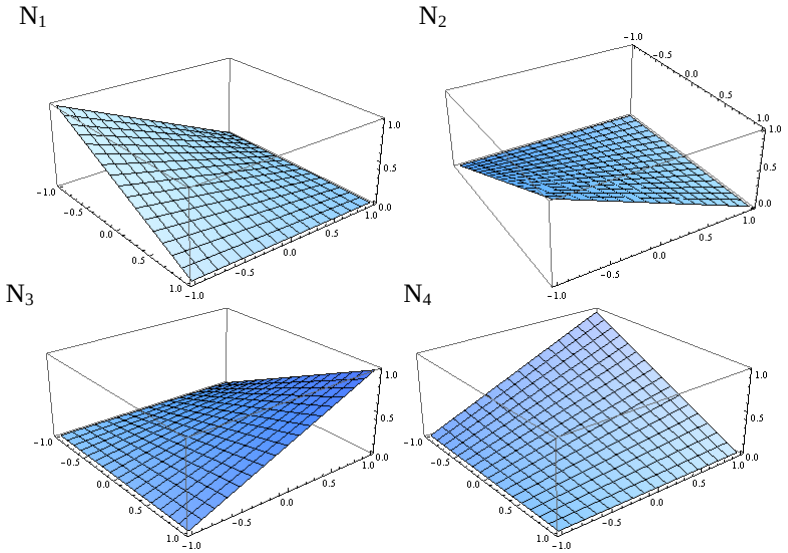

Fig. 6. Bilinear shape functions

The relation between the components of deformation within a finite element and its nodal displacements is described by the formula

$$\boldsymbol{\varepsilon} = \begin{bmatrix} \varepsilon_{11} \\ \varepsilon_{22} \\ 2\varepsilon_{12} \end{bmatrix} = \partial \mathbf{N}\mathbf{q} = \mathbf{B}\mathbf{q} \tag{5.2}$$

in which ∂ is the matrix operator of partial derivatives, $\mathbf{B}$ is the matrix of deformation compatibility consisting of the derivatives of shape functions N_i, and $\mathbf{q}^T = \left[u_1, v_1, u_2, v_2, u_3, v_3, u_4, v_4\right]$ is a vector of nodal displacements of the finite element. The displacement field within an element $\Omega_e \subset \Omega$ is expressed as

$$\mathbf{u} = \mathbf{N}\mathbf{q} \tag{5.3}$$

wherein

$$\mathbf{N} = \begin{bmatrix} N_1 & 0 & N_2 & 0 & N_3 & 0 & N_4 & 0 \\ 0 & N_1 & 0 & N_2 & 0 & N_3 & 0 & N_4 \end{bmatrix} \tag{5.4}$$

In modelling the components of microstructure, the linear elastic model of isotropic material was applied. For the isotropic elastic material being in the plain state of stress, the element stiffness matrix is defined by the formula

$$\mathbf{K}^e = \int_{\Omega_e} \mathbf{B}^T \mathbf{D}_i \mathbf{B} d\Omega \tag{5.5}$$

where

$$\mathbf{D}_i = \frac{E_i}{1-\nu_i^2} \begin{bmatrix} 1 & \nu_i & 0 \\ \nu_i & 1 & 0 \\ 0 & 0 & \dfrac{1-\nu_i}{2} \end{bmatrix} \tag{5.6}$$

and i = 1,2,3 is the number of the particular component of microstructure assigned to the finite element Ω_e.

The element stiffness matrix $\overline{\mathbf{D}}_E$ of the material on the macro scale is calculated by Eq. (5.5), in which a matrix $\overline{\mathbf{D}}$ is used instead of $\mathbf{D}_i$. The elasticity matrix $\overline{\mathbf{D}}$ of the homogenized material on the macro scale are determined by solving the boundary value problem on the micro scale for imposed components

of macro strain $\bar{\boldsymbol{\varepsilon}}$. A finite element formulation of the boundary value problem on the micro scale is considered next.

6. BOUNDARY VALUE PROBLEM

The boundary value problem of mechanics for the specified RVE after the FEM discretization is solved by the minimization of the elastic strain energy function with additional constraints

$$\min_{\mathbf{u}} \varphi(\mathbf{u}) = \frac{1}{2}\mathbf{u}^{\mathrm{T}}\mathbf{K}\mathbf{u} - \mathbf{u}^{\mathrm{T}}\mathbf{f} \qquad s.t. \quad \mathbf{C}\mathbf{u} - \mathbf{g} = \mathbf{0} \tag{6.1}$$

The minimization problem (6.1) can be solved by using the Lagrange multiplier method. However, due to a large computational complexity of the numerical homogenization method the approach based on Lagrange multipliers is too time consuming. Hence we follow an alternative approach [1, 3] that brings down to the solution of the equations:

$$\tilde{\mathbf{K}}\mathbf{u} = \tilde{\mathbf{F}} \tag{6.2}$$

where

$$\tilde{\mathbf{K}} = \mathop{\mathrm{A}}_{e}\left[(\mathbf{C}_u^e)^T\mathbf{C}_u^e + (\mathbf{Q}_u^e)^T\mathbf{K}^e\mathbf{Q}_u^e\right] \tag{6.3}$$

$$\tilde{\mathbf{F}} = \mathop{\mathrm{A}}_{e}\left[\mathbf{D}_u^e\bar{\boldsymbol{\varepsilon}}[(\mathbf{C}_u^e)^T - (\mathbf{Q}_u^e)^T\mathbf{K}^e\mathbf{R}_u^e]\right] \tag{6.4}$$

$$\mathbf{Q}_u^e = \mathbf{I} - \mathbf{R}_u^e\mathbf{C}_u^e \tag{6.5}$$

$$\mathbf{R}_u^e = (\mathbf{C}_u^e)^T[\mathbf{C}_u^e(\mathbf{C}_u^e)^T]^{-1} \tag{6.6}$$

In Eqns. (6.3) and (6.4) the symbol $\mathop{\mathrm{A}}_{e}$ means the finite element aggregation of matrices. To enforce deformations of RVE in accordance with the macro-deformations $\bar{\boldsymbol{\varepsilon}}$ there were applied the displacement boundary conditions of the first type

$$\mathbf{C}_u^e\mathbf{u} = \mathbf{D}_u^e\bar{\boldsymbol{\varepsilon}} = \mathbf{g}_u^e \tag{6.7}$$

where

$$\mathbf{C}_u^e = \int_{\Gamma}\mathbf{H}_u\mathbf{N}^T\mathbf{N}d\Gamma \tag{6.8}$$

$$\mathbf{D}_u^e = \int_\Gamma \mathbf{H}_u \mathbf{N}^T \mathbf{X} d\Gamma \tag{6.9}$$

The matrices $\mathbf{C}_u^e$, $\mathbf{D}_u^e$ and others involved in Eqns. (6.8) and (6.9) are given in explicit form in the Appendix. The master finite element $\Omega_e = (-1,1)\times(-1,1)$ together with definition of its boundary Γ used in analysis is presented in Fig. 7, whereas the way of integrating along the boundary in Eqn. (6.10).

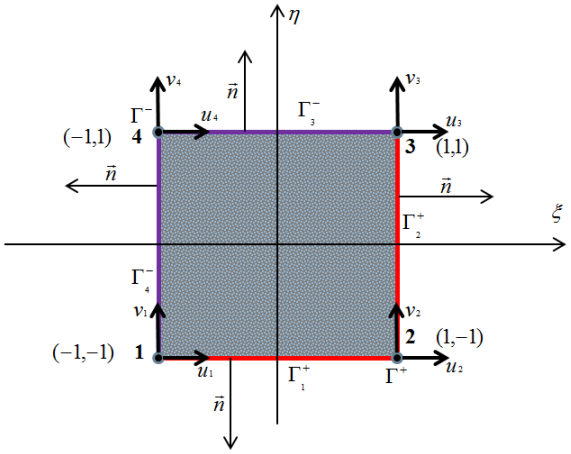

Fig. 7. Master finite element Q4

$$\begin{aligned}\int_\Gamma (\bullet)(\xi,\eta)d\Gamma = &\int_{-1}^{1} (\bullet)(\xi,-1)d\xi + \int_{-1}^{1} (\bullet)(1,\eta)d\eta \\ &+ \int_{-1}^{1} (\bullet)(\xi,1)d\xi + \int_{-1}^{1} (\bullet)(-1,\eta)d\eta\end{aligned} \tag{6.10}$$

7. NUMERICAL EXAMPLES

In this section we present the results of numerical tests we obtained as the solution of the boundary value problem on micro-scale for the RVE shown in Fig. 14. However, let us begin with tests checking the response of homogeneous isotropic material to some imposed macro-strains. The forms of deformation (lighter line) of one homogeneous element due to the enforced macro-deformations $\overline{\boldsymbol{\varepsilon}}$, with

values given therein, are displayed in Fig. 8. Test results for a homogenous isotropic material and 5x5 finite element mesh are shown in Figs. 9 – 12 (deformed grids in darker line). As can be seen the obtained results confirm the expected deformation modes of RVE. Figure 13 shows the distribution of micro-stresses induced by sheering $\bar{\boldsymbol{\varepsilon}}^{\mathrm{T}} = [0 \quad 0 \quad 1]$ for three microstructures of two-component material with isotropic components of parameters E_1=20 GPa, ν_1=0.4, E_2=200 GPa, ν_2=0.4, and the 10x10 grid RVE.

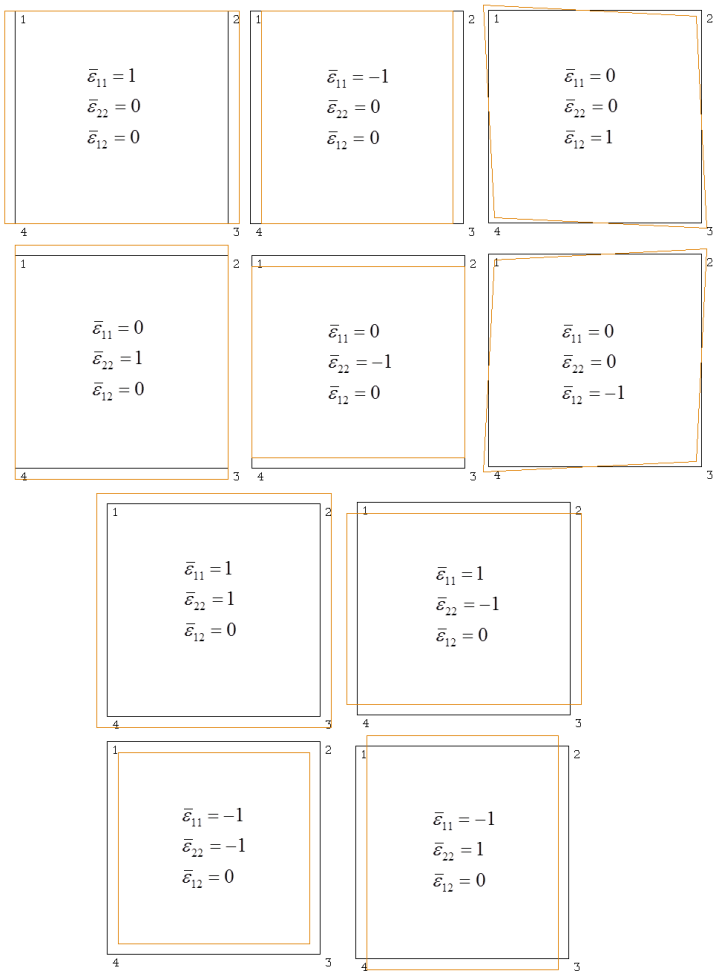

Fig. 8. Deformation tests on single-element homogeneous cell

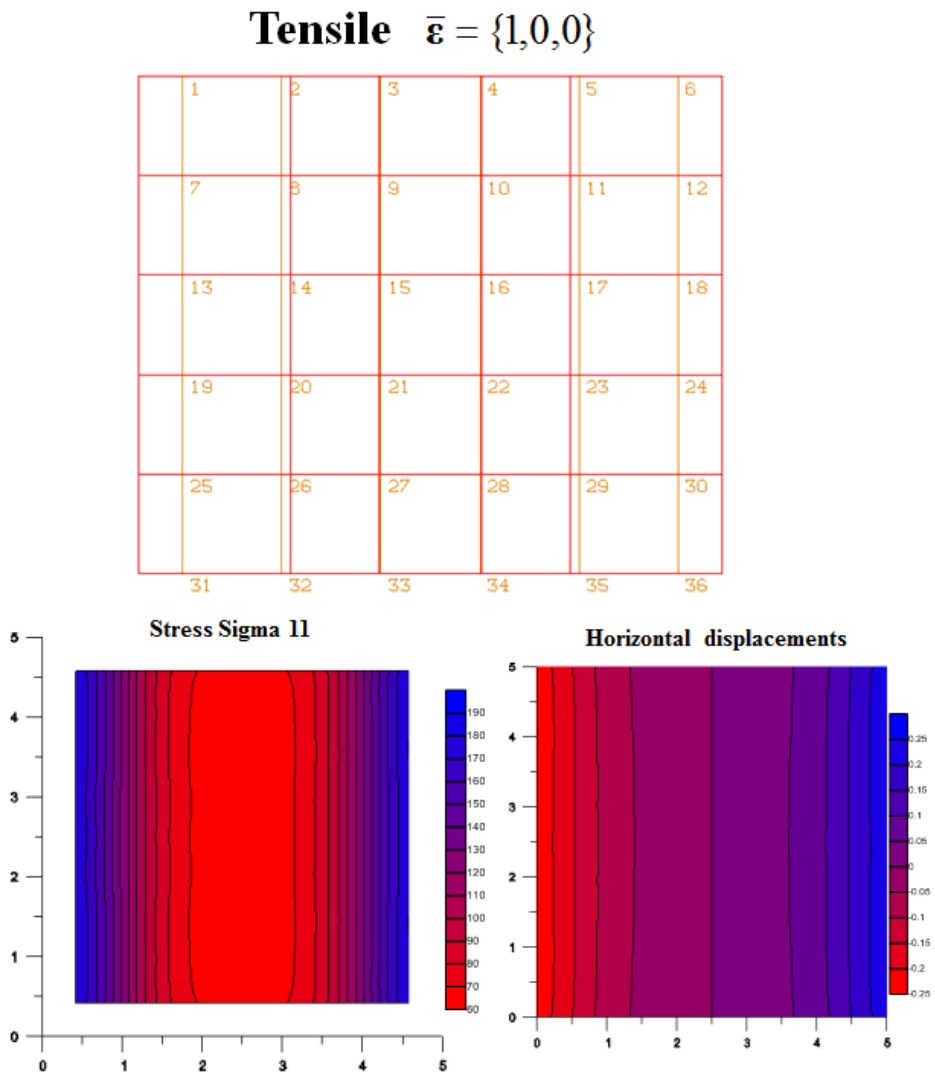

Fig. 9. Tensile test for a homogenous material, deformed finite element mesh in dark line

Finally, Fig. 14 shows the distribution of stresses in a randomly generated microstructure of RPC composed of cement matrix (47.08%), crushed quartz (8.4%), sand (40.52%) and pores (4%). The used values of material parameters: cement matrix E=30 GPa, ν=0.16, crushed quartz and sand E=75 GPa, ν=0.3. The RVE was divided into 50x50 finite elements. The macro-strain imposed on the boundary of RVE was $\bar{\varepsilon} = \{-1,0.2,0\}$.

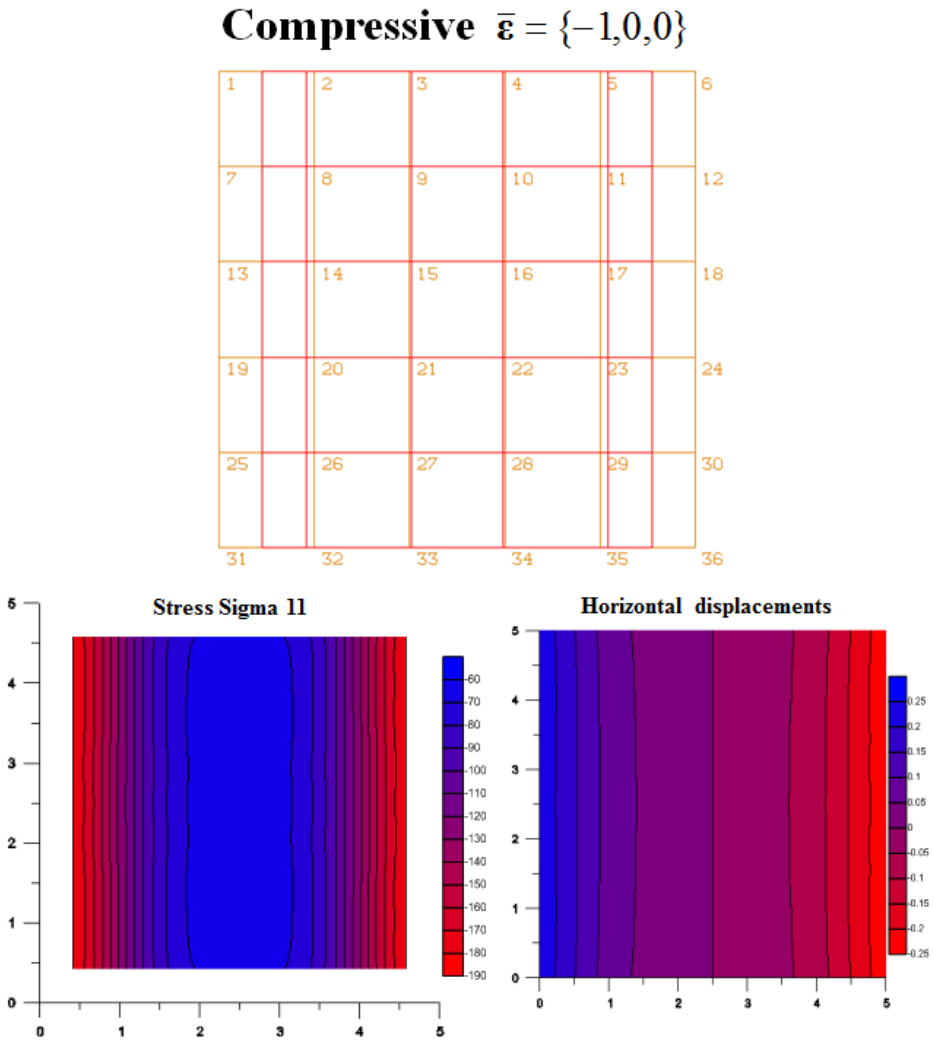

Fig. 10. Compressive test for a homogenous material, deformed finite element mesh in dark line

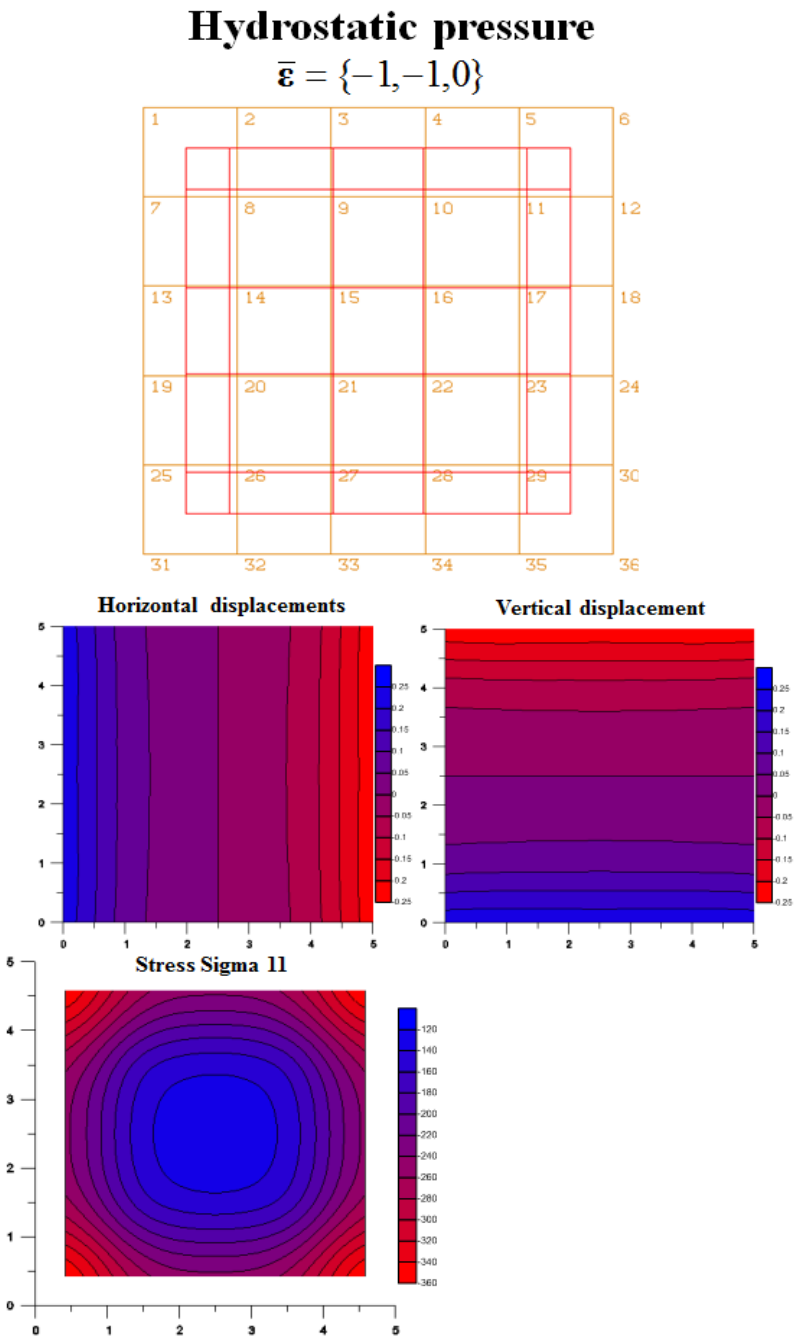

Fig. 11. Hydrostatic pressure test for a homogenous material, deformed finite element mesh in dark line

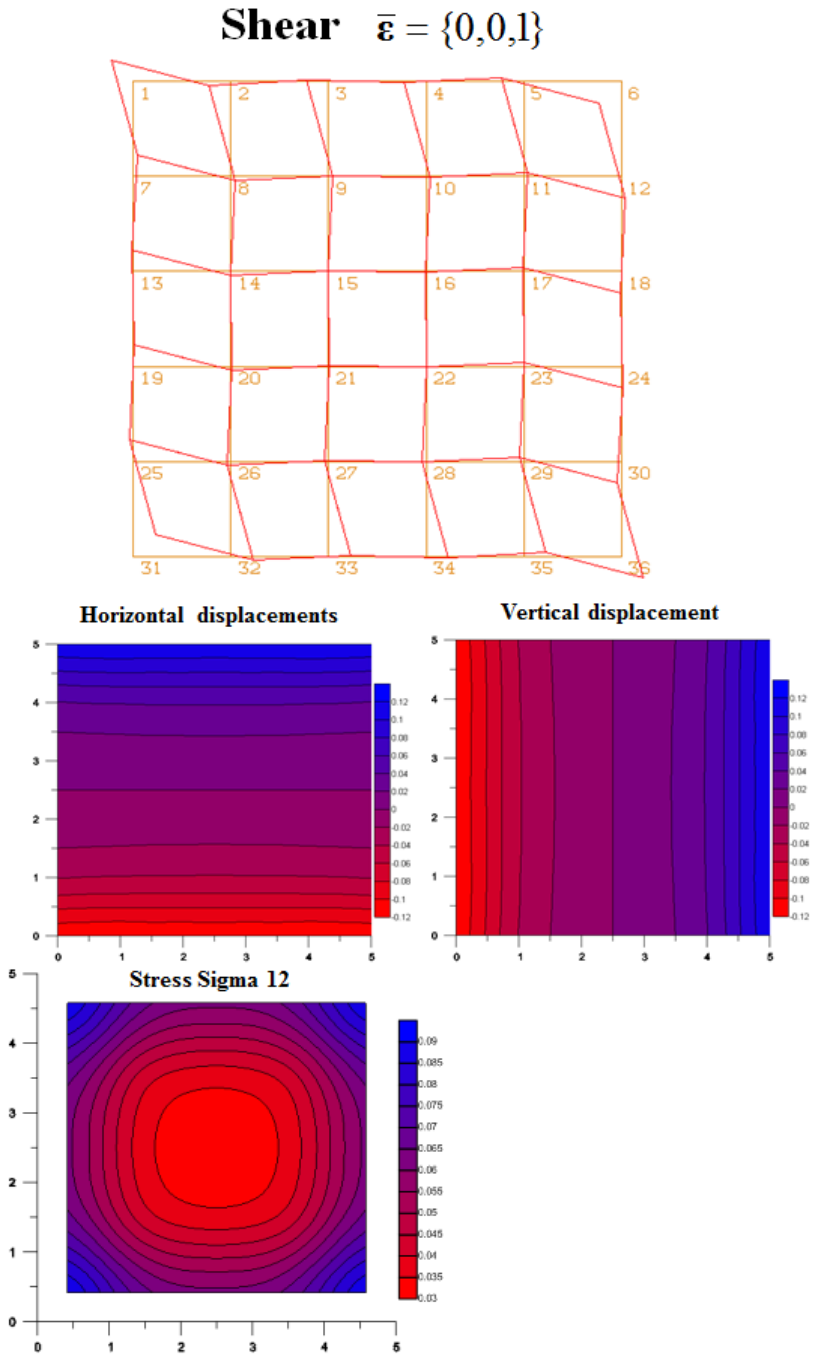

Fig. 12. Shear test for a homogenous material

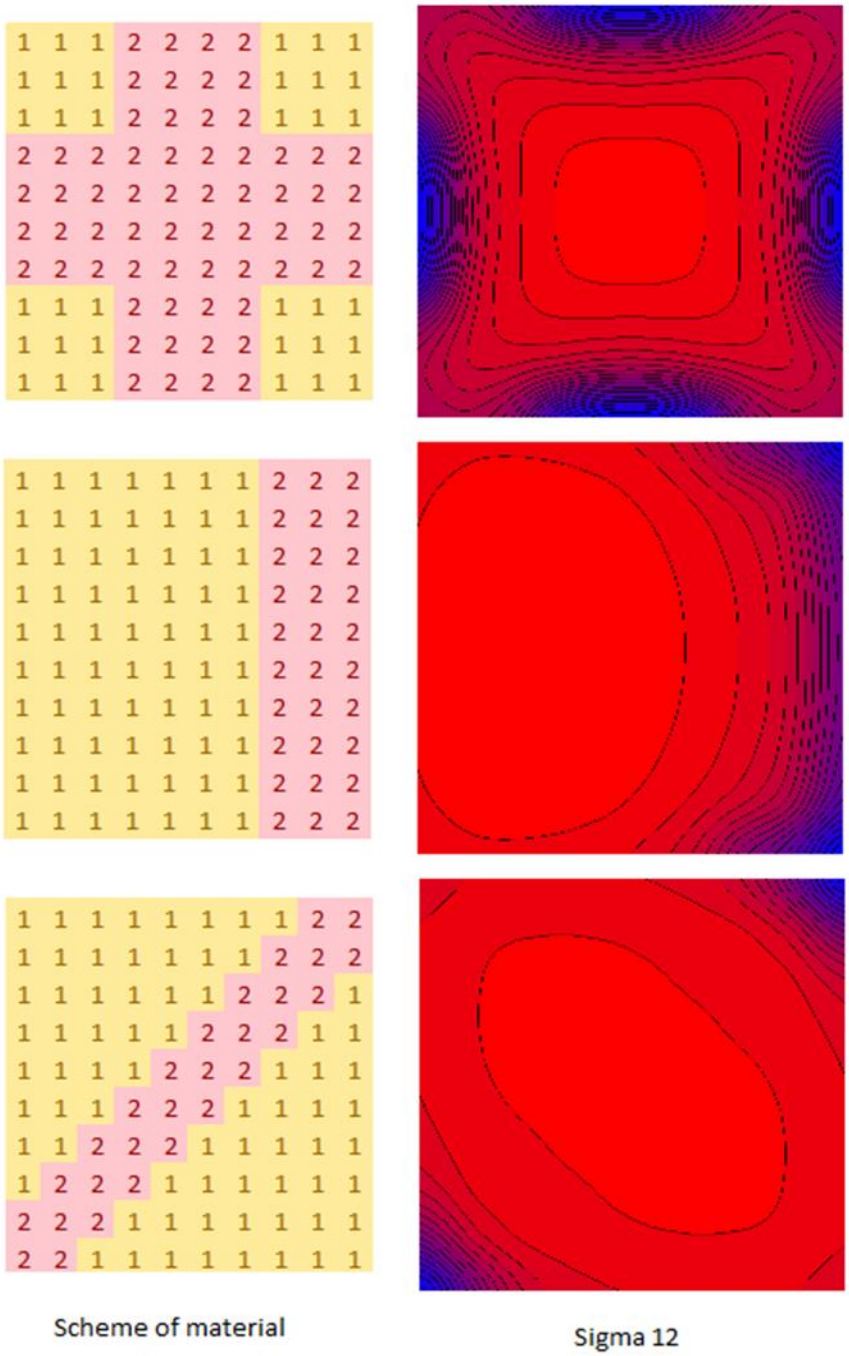

Fig. 13. Shear test for a heterogeneous material

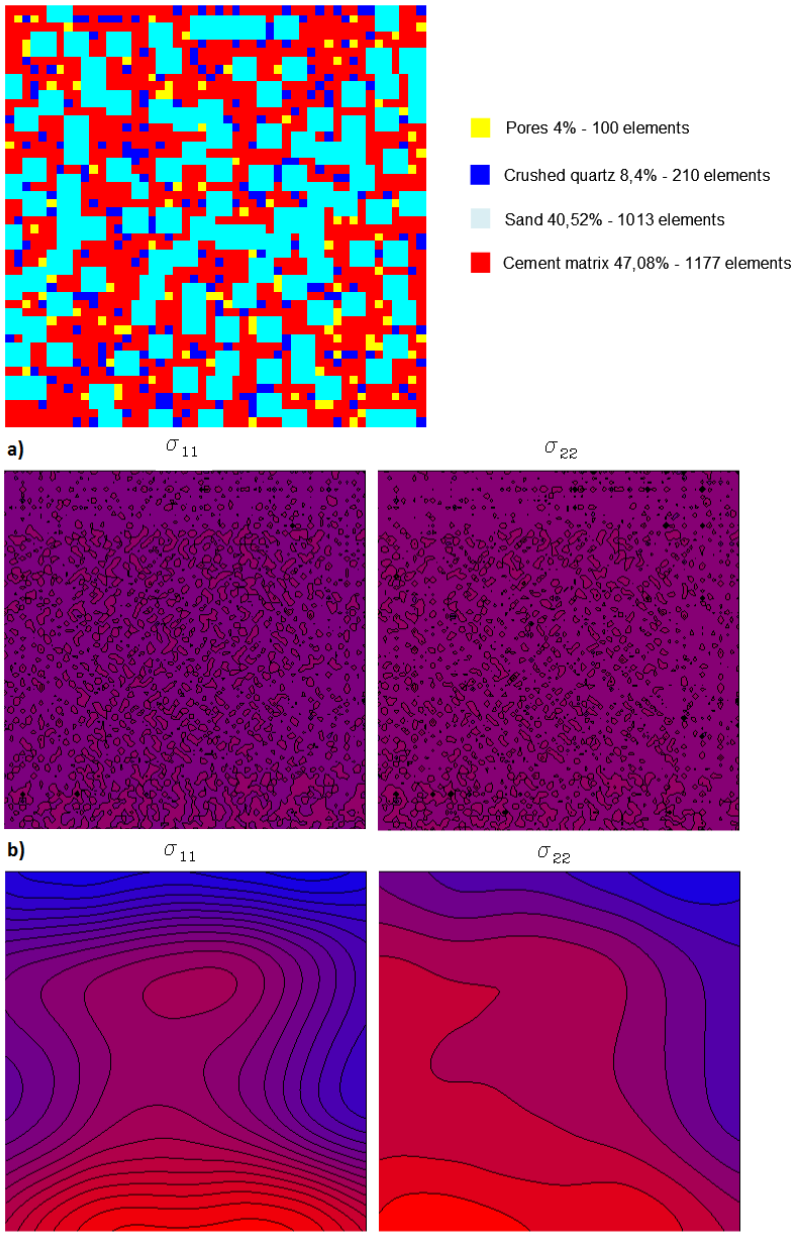

Fig. 14. Microstructure of the RVE, a) micro-stress distribution and b) smoothed micro-stress distribution induced by macro-strain $\bar{\boldsymbol{\varepsilon}} = \{-1{,}0.2{,}0\}$

8. CLOSING REMARK

A two-scale numerical approach to the modelling of reactive powder concrete (RPC) was presented, in which the layout of microstructure (2D case) is generated randomly for a given composition of RPC. The boundary value problem on representative volume element (RVE) was solved for the case of imposed (given) macro-strains on the boundary of RVE. A computer program was developed and herein results of some numerical tests are included. In the next part of the work, results of a fully two-scale analysis will be presented as well as results of our own laboratory tests curried out on cubes and beams made of RPC.

ACKNOWLEDGEMENTS

The first author is a scholar within Sub-measure 8.2.2 Regional Innovation Strategies, Measure 8.2 Transfer of knowledge, Priority VIII Regional human resources for the economy Human Capital Operational Programme co-financed by European Social Fund and state budget.

REFERENCES

1. Ainsworth M.: Essential boundary conditions and multi-point constraints in finite element analysis, *Comput. Methods Appl. Mech. Engrg*. 190 (2001) 6323 - 6339.
2. Jasiczak J., Wdowska A., Rudnicki T.: *Betony ultrawysokowartościowe. Właściwości, technologie, zastosowania*, Stowarzyszenie Producentów Cementu, Kraków 2008.
3. Kaczmarczyk Ł.: *Numeryczna analiza wybranych problemów mechaniki ośrodków niejednorodnych*, PhD thesis, Cracow University of Technology 2006.
4. Kouznetsova V.G., Geers M.G.D., Brekelmans W.A.M.: Multi-scale second-order computational homogenization of multi-phase materials: a nested finite element solution strategy, *Comput. Methods Appl. Mech. Engrg*. 193 (2004) 5525 - 5550.
5. Miehe C.: Computational micro-to-macro transitions for discretized micro-structures of heterogeneous materials at finite strains based on the minimization of averaged incremental energy, *Comput. Methods Appl. Mech. Engrg*. 192 (2003) 559 - 591.
6. Zdeb T., Śliwiński J.: Beton z proszków reaktywnych – właściwości mechaniczne i mikrostruktura, *Budownictwo Technologie Architektura* 51 (2010) 51 - 55.
7. DISLIN Scientific Plotting Software http://www.mps.mpg.de/dislin/
8. SLATEC A Mathematical Library http://www.netlib.org/slatec/index.html
9. http://www.ductal-lafarge.com/

DWUSKALOWY MODEL BETONU Z PROSZKÓW REAKTYWNYCH.
CZĘŚĆ I: REPREZENTATYWNY ELEMENT OBJĘTOŚCIOWY (RVE)
I ROZWIĄZANIE ZAGADNIENIA BRZEGOWEGO NA RVE

S t r e s z c z e n i e

Artykuł jest pierwszą częścią pracy dotyczącej modelowaniu betonów z proszków reaktywnych przy zastosowaniu numerycznej homogenizacji. Technika ta jest podejściem wielkoskalowego modelowania. W tym konkretnym przypadku modelowania dwuskalowego. Zachowanie modelu betonu typu RPC w skali makro (skala punktu materialnego, poziom opisu fenomenologicznego) opisywane jest na podstawie zjawisk zachodzących w mikrostrukturze materiału (mikroskala). Takie podejście daje możliwość uwzględnienia szeregu zjawisk zachodzących w mikrostrukturze na właściwości fizyczne i mechaniczne materiału. Na przykład wpływ mikropęknięć na wytrzymałość betonu. Nie bez znaczenia jest fakt, że metoda nie wymaga znajomości równań konstytutywnych w skali makro, związki te są wyznaczane w sposób niejawny dla każdego przyrostu obciążenia na podstawie numerycznego modelu reprezentatywnego elementu objętościowego RVE. Do wyznaczenia niejawnych związków fizycznych w makroskali niezbędna jest znajomość geometrii mikrostruktury, równań konstytutywnych na poziomie skali mikro oraz ich parametrów. W tej pierwszej części pracy ograniczono się do sformułowania i rozwiązania zagadnienia brzegowego na poziomie mikroskali dla zadanych makronaprężeń na brzegu RVE. Opracowano własny program komputerowy, który generuje w sposób losowy mikrostrukturę RPC i rozwiązuje problem brzegowy zdyskretyzowany metodą elementów skończonych. Praca zawiera wyniki obliczeń zadań testowych.

APPENDIX

Matrix $\mathbf{C}_u^e$, $\mathbf{D}_u^e$ for displacement boundary conditions where x_i and y_i i = 1,2,3,4 are coordinates of nodes in the global coordinate system.

$$\mathbf{H}_u = \operatorname{diag}\begin{bmatrix}1 & 1 & 1 & 1 & 1 & 1 & 1 & 1\end{bmatrix} \qquad \mathbf{X} = \frac{1}{2}\begin{bmatrix}2\xi & 0 & \eta \\ 0 & 2\eta & \xi\end{bmatrix}$$

$$\mathbf{J} = \begin{bmatrix} \frac{1}{4}\left[(\eta-1)x_1 - (\eta-1)x_2 + (\eta+1)(x_3 - x_4)\right] & \frac{1}{4}\left[(\eta-1)y_1 - (\eta-1)y_2 + (\eta+1)(y_3 - y_4)\right] \\ \frac{1}{4}\left[(\xi-1)x_1 - (\xi+1)x_2 + \xi x_3 - \xi x_4 + x_3 + x_4\right] & \frac{1}{4}\left[(\xi-1)y_1 - (\xi+1)y_2 + \xi y_3 - \xi y_4 + y_3 + y_4\right] \end{bmatrix}$$

$$\mathbf{C}_u^e = \int_\Gamma \mathbf{H}_u \mathbf{N}^{\mathrm{T}} \mathbf{N} \cdot \det|\mathbf{J}| d\Gamma = \int_{-1}^{1} \mathbf{H}_u \mathbf{N}^{\mathrm{T}}(\xi,-1)\mathbf{N}(\xi,-1) \cdot \det|\mathbf{J}| d\xi +$$
$$\int_{-1}^{1} \mathbf{H}_u \mathbf{N}^{\mathrm{T}}(1,\eta)\mathbf{N}(1,\eta) \cdot \det|\mathbf{J}| d\eta + \int_{-1}^{1} \mathbf{H}_u \mathbf{N}^{\mathrm{T}}(\xi,1)\mathbf{N}(\xi,1) \cdot \det|\mathbf{J}| d\xi +$$
$$\int_{-1}^{1} \mathbf{H}_u \mathbf{N}^{\mathrm{T}}(-1,\eta)\mathbf{N}(-1,\eta) \cdot \det|\mathbf{J}| d\eta$$

$$\mathbf{C}_u^e = \begin{bmatrix} C_1 & 0 & C_2 & 0 & 0 & 0 & C_3 & 0 \\ & C_1 & 0 & C_2 & 0 & 0 & 0 & C_3 \\ & & C_4 & 0 & C_5 & 0 & 0 & 0 \\ & & & C_4 & 0 & C_5 & 0 & 0 \\ & & & & C_6 & 0 & C_7 & 0 \\ & & \textit{sym.} & & & C_6 & 0 & C_7 \\ & & & & & & C_8 & 0 \\ & & & & & & & C_8 \end{bmatrix}$$

$$C_1 = \frac{1}{24}\left(x_4(7y_1 - 6y_2 - y_3) + (7x_1 - x_3)(y_2 - y_4) + x_2(-7y_1 + y_3 + 6y_4)\right)$$

$$C_2 = \frac{1}{24}(x_4y_1 + x_3(y_1 - y_2) + 2x_1y_2 - x_4y_2 - x_1y_3 - x_1y_4 + x_2(-2y_1 + y_3 + y_4))$$

$$C_3 = \frac{1}{24}(2x_4y_1 + x_1y_2 - x_4y_2 + x_1y_3 - x_4y_3 - 2x_1y_4 + x_2(y_4 - y_1) + x_3(y_4 - y_1))$$

$$C_4 = \frac{1}{24}(x_4y_1 + 7x_1y_2 - 7x_2(y_1 - y_3) - 6x_1y_3 - x_4y_3 - x_1y_4 + x_3(6y_1 - 7y_2 + y_4))$$

$$C_5 = \frac{1}{24}((x_1 + x_4)(y_2 - y_3) + x_3(y_1 - 2y_2 + y_4) - x_2(y_1 - 2y_3 + y_4))$$

$$C_6 = \frac{1}{24}(x_4(y_1 + 6y_2 - 7y_3) + (x_1 - 7x_3)(y_2 - y_4) - x_2(y_1 - 7y_3 + 6y_4))$$

$$C_7 = \frac{1}{24}(x_4(y_1 + y_2 - 2y_3) + (x_1 + x_2)(y_3 - y_4) - x_3(y_1 + y_2 - 2y_4))$$

$$C_8 = \frac{1}{24}(7x_4y_1 + x_1y_2 + 6x_1y_3 - 7x_4y_3 + x_2(y_3 - y_1) - 7x_1y_4 - x_3(6y_1 + y_2 - 7y_4))$$

$$\mathbf{D}_u^e = \int_\Gamma \mathbf{H}_u \mathbf{N}^T \mathbf{X} \cdot \det|\mathbf{J}| d\Gamma = \int_{-1}^{1} \mathbf{H}_u \mathbf{N}^T(\xi,-1)\mathbf{X}(\xi,-1) \cdot \det|\mathbf{J}| d\xi +$$
$$\int_{-1}^{1} \mathbf{H}_u \mathbf{N}^T(1,\eta)\mathbf{X}(1,\eta) \cdot \det|\mathbf{J}| d\eta + \int_{-1}^{1} \mathbf{H}_u \mathbf{N}^T(\xi,1)\mathbf{X}(\xi,1) \cdot \det|\mathbf{J}| d\xi +$$
$$\int_{-1}^{1} \mathbf{H}_u \mathbf{N}^T(-1,\eta)\mathbf{X}(-1,\eta) \cdot \det|\mathbf{J}| d\eta$$

$$\mathbf{D}_u^e = \begin{bmatrix} D_1 & 0 & D_5 \\ 0 & D_5 & D_1 \\ D_2 & 0 & D_6 \\ 0 & D_6 & D_2 \\ D_3 & 0 & D_7 \\ 0 & D_7 & D_3 \\ D_4 & 0 & D_8 \\ 0 & D_8 & D_4 \end{bmatrix}$$

$$D_1 = \frac{1}{12}(-4x_4y_1 - 3x_1y_2 + 3x_4y_2 - x_1y_3 + x_4y_3 + 3x_2(y_1 - y_4) + x_3(y_1 - y_4) + 4x_1y_4)$$

$$D_2 = \frac{1}{12}((3x_1 + x_4)(y_2 - y_3) + x_3(3y_1 - 4y_2 + y_4) - x_2(3y_1 - 4y_3 + y_4))$$

$$D_3 = \frac{1}{12}((x_1 + 3x_4)(y_2 - y_3) + x_3(y_1 - 4y_2 + 3y_4) - x_2(y_1 - 4y_3 + 3y_4))$$

$$D_4 = \frac{1}{12}(-4x_4y_1 - x_1y_2 + x_4y_2 - 3x_1y_3 + 3x_4y_3 + x_2(y_1 - y_4) + 3x_3(y_1 - y_4) + 4x_1y_4)$$

$$D_5 = \frac{1}{12}\big(-3x_4y_1 - 4x_1y_2 + 3x_4y_2 + x_3(y_2 - y_1) + x_1y_3 + 3x_1y_4 + x_2(4y_1 - y_3 - 3y_4)\big)$$

$$D_6 = \frac{1}{12}(-x_4y_1 - 3x_3(y_1 - y_2) - 4x_1y_2 + x_4y_2 + 3x_1y_3 + x_2(4y_1 - 3y_3 - y_4) + x_1y_4)$$

$$D_7 = \frac{1}{12}\big(x_4(y_1 + 3y_2 - 4y_3) + (x_1 + 3x_2)(y_3 - y_4) - x_3(y_1 + 3y_2 - 4y_4)\big)$$

$$D_8 = \frac{1}{12}\big(x_4(3y_1 + y_2 - 4y_3) + (3x_1 + x_2)(y_3 - y_4) - x_3(3y_1 + y_2 - 4y_4)\big)$$